

## Polyoxometalate-assisted Metal Nanomaterials Synthesis<sup>#</sup>

Ji Hyun Seog,<sup>†</sup> Dongheun Kim,<sup>†,‡</sup> Sang Woo Han,<sup>‡</sup> and Sang Bok Lee<sup>†,§,\*</sup>

<sup>†</sup>Graduate School of Nanoscience and Technology, Korea Advanced Institute of Science and Technology, Daejeon 305-701, Korea. \*E-mail: slee@umd.edu

<sup>‡</sup>Department of Chemistry and KI for the NanoCentury, Korea Advanced Institute of Science and Technology, Daejeon 305-701, Korea

<sup>§</sup>Department of Chemistry and Biochemistry, University of Maryland, College Park, MD 20742, USA  
Received October 31, 2014, Accepted December 18, 2014, Published online February 20, 2015

In this review, we present the polyoxometalate (POM)-mediated synthesis of nanomaterials and their performance as catalysts. Various nanomaterials have been successfully synthesized in a facile process using POMs as a reducing and stabilizing agent. The reduction of metal ions was effected by the reduced POMs, which converted their oxidation state without structural change. The presence of POMs on the nanomaterials was confirmed through a variety of analytical methods. The alteration of the size and morphology of nanomaterials was observed to be controlled by the molar ratio of metal salt to the POMs. The synthesized nanomaterials showed good catalytic activity, which could be used as multifunctional catalysts.

**Keywords:** Polyoxometalate, Nanoparticle, Nanohybrid, Catalyst

### Introduction

Polyoxometalates (POMs) are one class of widely used early transition-metal oxygen cluster anions with potential for use in various applications in materials science,<sup>1,2</sup> catalysis,<sup>3,4</sup> and medicine.<sup>5</sup> POMs have a variety of structures including the Lindqvist [M<sub>6</sub>O<sub>19</sub>]<sup>−</sup>, Anderson [XM<sub>6</sub>O<sub>24</sub>]<sup>n−</sup>, Keggin [XM<sub>12</sub>O<sub>40</sub>]<sup>n−</sup>, and Wells–Dawson [X<sub>2</sub>M<sub>18</sub>O<sub>62</sub>]<sup>n−</sup>, where X is a heteroatom such as P, Si, As, or Ge; M is a metal, such as Mo, V, W, or Nb; and *n* is the overall charge (Figure 1). They possess fascinating properties, such as high thermal stability, high hydrolytic stability, Lewis acidity, strong Brønsted acidity, photocatalytic activity, and reversible redox activity.<sup>6–8</sup> The first synthesized POM was reported in the early 19th century, and the number of publications and patents concerning POM chemistry and technology has gradually grown during the 20th century.<sup>1,9</sup>

The synthesis of nanomaterials has been an important field of research over the past few decades, because nanomaterials have unique chemical, physical, and electrical properties arising from their nanometer length scale, as compared to their bulk materials;<sup>10,11</sup> consequently, they have great potential for application in various fields, such as catalysis, electronics, semiconductors, drug delivery, imaging agents, and so on.<sup>12–16</sup>

In recent years, POMs have been introduced for use in the synthesis of nanomaterials as reducing and stabilizing agents, and these synthetic methods have been proposed in many publications. POMs can be reduced photochemically,<sup>17</sup> electrochemically,<sup>18</sup> or radiochemically,<sup>19</sup> or using suitable chemical reducing reagents<sup>20</sup> without decomposition or

change in their structural configuration; the reduced POMs then have the capability to reduce metal ions.<sup>21,22</sup> The synthesized nanomaterials present negative charges due to the presence of POMs on their surface, which can prevent aggregation of the nanomaterials by electrostatic repulsion, enabling long-term stability.<sup>23</sup> Moreover, POMs are suitable candidates for green chemistry, owing to their recyclability and reusability during the redox process for the green synthesis of nanomaterials in aqueous systems.<sup>24,25</sup>

In this review, we present recent research on the formation of various nanomaterials by using POMs as reducing and stabilizing agents. We also introduce methods for the synthesis of a POM-mediated nanohybrid in the several studies and their synergetic effects in catalytic reactions, showing potential applications of POMs.

### Synthesis of Monometallic Nanomaterials by POMs

Many studies have reported the preparation of nanoparticles (NPs) by using POMs. In the synthesis of NPs, POMs can participate as agents for both reducing and stabilizing the NPs or just as stabilizing agents. Reduced POMs can be obtained photochemically, electrochemically, or radiochemically, or by using suitable chemical reducing reagents. Above all, the photochemical reduction strategy, which was first reported by Chakley in 1952, has been generally used for the synthesis of NPs.<sup>17</sup> As shown in Figure 2, POMs are reduced in the presence of sacrificial organic electron donors, which are oxidizable substrates, such as alcohol or organic pollutants, under UV irradiation and then the reduced POMs also reduce metal ions to their zero-state form.

**Silver Nanomaterials.** Various silver nanomaterials have been fabricated in the presence of POMs, as shown in

<sup>#</sup> This paper is dedicated to Professor Kwan Kim on the occasion of his honorable retirement.

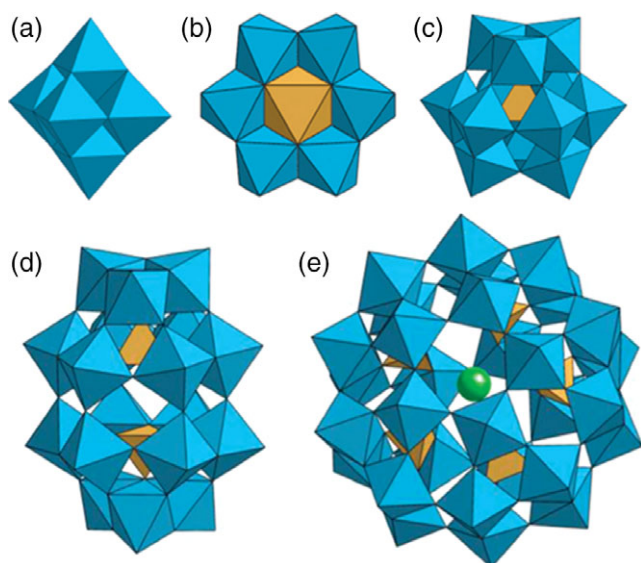


**Figure 1.** POM representations of (a) Lindqvist, (b) Anderson, (c) Keggin, (d) Wells–Dawson, and (e) Preyssler polyoxoanions. The blue octahedrons confirm the metal oxide core. Adopted from Ref. 7 with permission from the Royal Society of Chemistry.



**Figure 2.** Polyoxometalate-assisted photocatalytic cycle for the reduction of a transition or noble metal ion to nanomaterials.

Figure 3. Papaconstantinou and coworkers produced silver NPs using photochemically reduced Keggin-type POMs, which served as a photocatalyst, reducing agent, and stabilizing agent in this aqueous system (Figure 3(a)). They also achieved the synthesis of Au, Pd, and Pt NPs in the same way.<sup>26</sup>

Nadjo and coworkers reported that silver NPs could be altered from spherical to twisted helical NPs by controlling the reducing power of POMs (Figure 3(b) and (c)).<sup>27</sup> Mo<sup>V</sup>–Mo<sup>VI</sup> mixed-valence POMs were used as a reducing agent, stabilizing agent, and shape controller in this study. Spherical NPs were formed with the more rapid reduction of silver ions by using POMs with strong reducing power, and the size of the spherical NPs was tunable in accordance with the molar ratio of the metal ions to POMs (Figure 3(b)); the twisted helical nanowires were fabricated through a relatively slow reduction process by the POMs with weak reducing power (Figure 3(c)). The synthesized NPs did not show aggregation for a long time, and TEM images showed that the POMs covered the surface of the NPs. These results indicate the POMs can effectively stabilize the NPs.

In another study, crystalline nanosaws and one-dimensional (1D) nanostructures were synthesized in the presence of three types of vanadium-substituted POMs, in which each POM was different with respect to the location and the number of vanadium elements (Figure 3(d)–(f)).<sup>28</sup> The formation of 1D

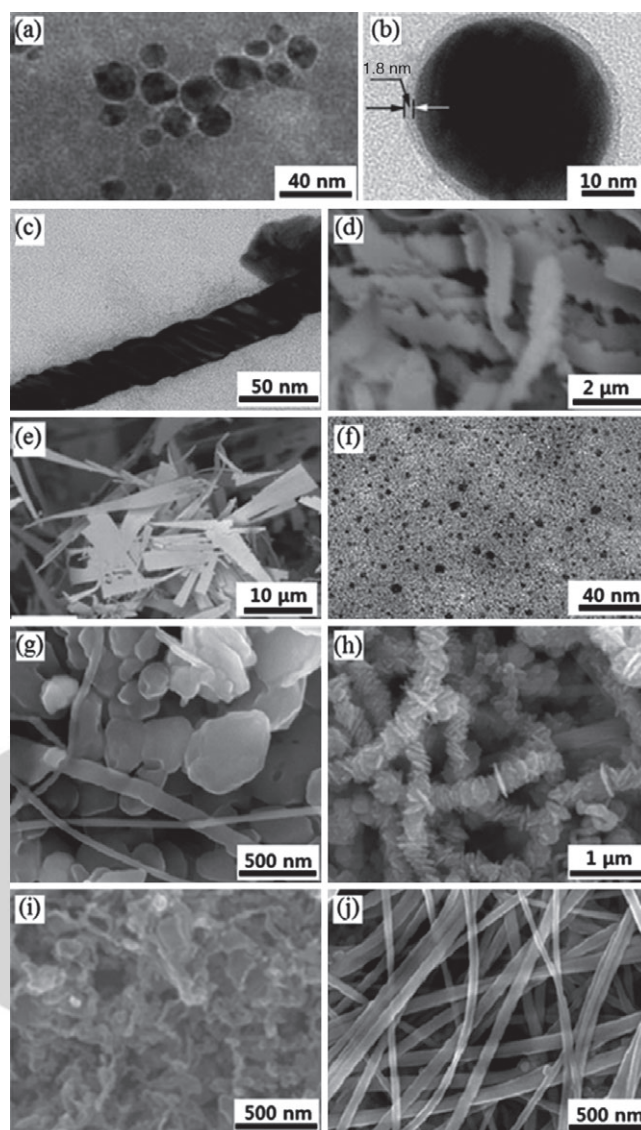


**Figure 3.** POM-assisted Ag nanomaterials. TEM images of (a) NPs,<sup>26</sup> (b) a magnified spherical NP, and (c) a twisted helical nanowire.<sup>27</sup> SEM images of (d) nanoribbons with saws on both sides of the ribbons and (e) nanosaws. (f) TEM image of spherical NPs.<sup>28</sup> SEM images of (g) nanoflakes and (h) nanoplates, and (i) nanobelts, and (j) nanowires.<sup>29</sup> Adapted with permission from the Wiley, the American Chemical Society, and the Royal Society of Chemistry.

nanostructures was caused by the agglomeration of spherical silver NPs at room temperature in all systems that used the three types of POMs. When the concentration of silver ions in the reaction solution was low, nanoribbons were formed (Figure 3(d)). However, a high concentration of silver ions in the reaction solution was favorable for the formation of nanosaws (Figure 3(e)). With a decrease in temperature, the spherical silver NPs did not participate in the aggregation process, and the formation of 1D nanostructures consequently did not occur (Figure 3(f)). In this study, POMs served a crucial role in the formation of 1D nanostructures and acted as a reducing agent, but the mechanism of formation has remained unclear.

Liu *et al.* investigated the influence of the reaction temperature, UV exposure time, concentration of reactants, and metal salt/POM molar ratio on the preparation of silver nanowires.<sup>29</sup> Various silver nanomaterials, such as silver nanoflakes, nanoplates, nanobelts, and nanowires, were synthesized by adjusting the reaction conditions in the presence of POMs (Figure 3(g)–(j)). With a low initial concentration of POMs, the formation of nanoflakes was preferred over that of nanowires due to the slow reaction. Likewise, the formation of nanowires was not observed at high concentrations of POMs because the formation of decahedral Ag seeds for growing nanowires was avoided, and selective interaction was prevented by coating of the entire surface of seeds.

**Gold Nanomaterials.** Spherical gold NPs were synthesized through photocatalytic reduction, as mentioned above (Figure 4(a)),<sup>26</sup> and the formation of various gold nanostructures in the presence of POMs was reported in addition to spherical shapes.

Highly faceted, multiply twinned gold NPs were fabricated with chemically reduced POMs (Figure 4(b)–(d)).<sup>20</sup> The

electrons were transferred from L-ascorbic acid to gold ions via POMs in this process, and the synthesized hexagonal or icosahedral NPs were stabilized by POMs, which was confirmed through X-ray diffraction (XRD) analysis. The morphology of the NPs was influenced by the reaction temperature, and highly faceted NPs were produced at high temperature, but the detailed mechanism was not identified. The synthesized NPs showed an enhanced electrocatalytic property toward the hydrogen evolution reaction.

Also, gold NPs with a controllable morphology were reported.<sup>30</sup> Multifarious nanomaterials, such as spherical NPs, triangular or hexagonal nanoplates, and twisted nanowires were synthesized by adjusting the concentrations of each composition and the molar ratio between the metal salt and POMs, where mixed-valence POMs acted as both a reductant and a stabilizing agent (Figure 4(e)–(g)). The shapes of the nanomaterials were seen to be affected by the molar ratio of metal salt to POMs. When the molar ratio was decreased to <1, the spherical NPs were changed to polygonal nanoplates, such as triangular and hexagonal shapes. On the other hand,

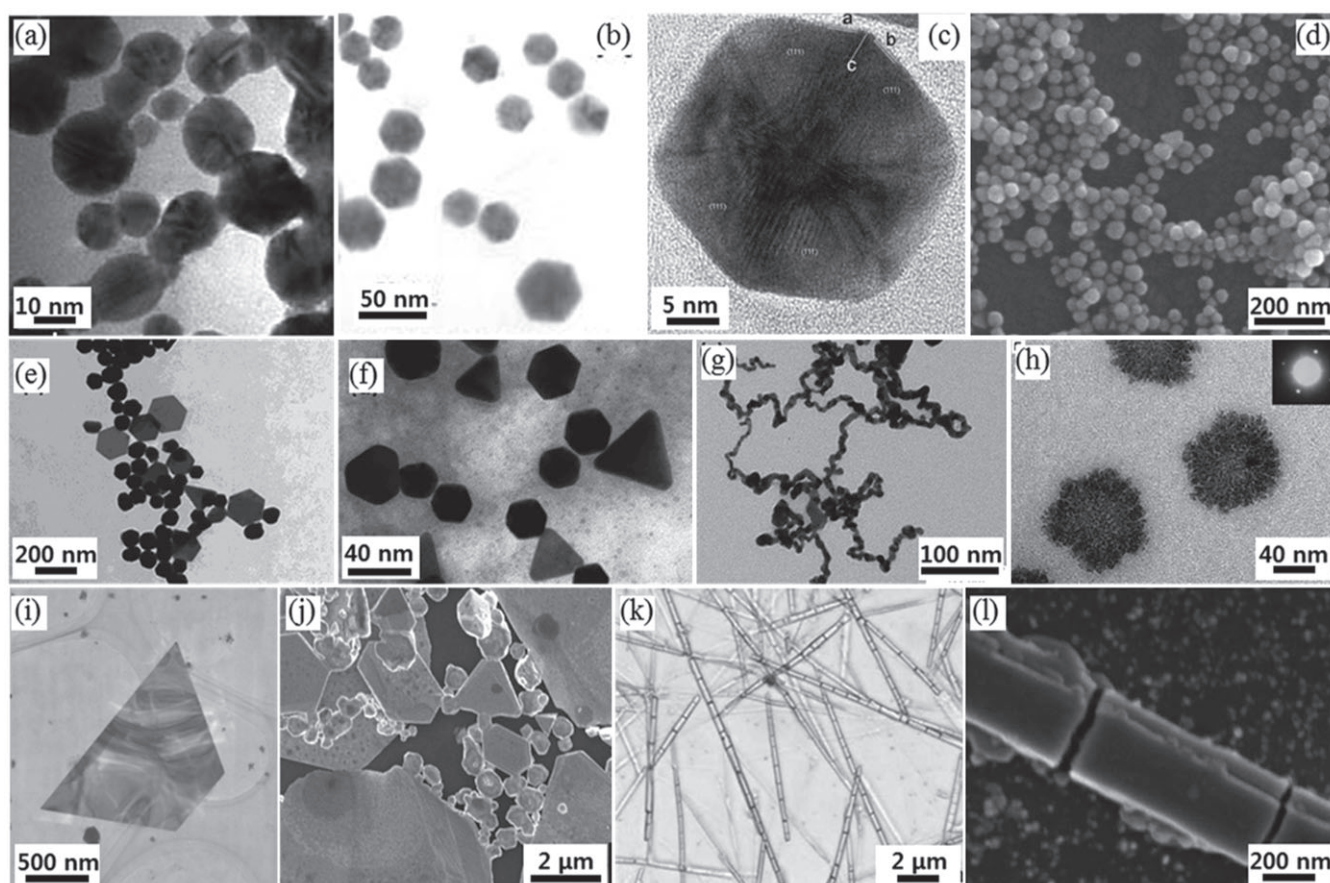


**Figure 4.** POM-assisted Au nanomaterials. TEM images of (a) spherical NPs,<sup>26</sup> (b) hexagonal NPs, and (c) a magnified hexagonal NP and the distribution of {111} facets. a, b are labeled as the *d*-spacing of a {111} facet, and c is labeled as a typical twin boundary between {111} facets. (d) Low-magnification SEM image of icosahedral NPs.<sup>20</sup> TEM images of (e) triangular and hexagonal nanoplates, (f) polygon-shaped nanomaterials including triangles and hexagons with some nanoplates, (g) twisted nanowires,<sup>30</sup> and (h) flower-like NPs. The inset displays the electron diffraction pattern<sup>31</sup> and (i) a nanosheet. (j) SEM image of sheets on a Si substrate.<sup>32</sup> TEM and SEM images of bamboo joint-like Au micro/nanostructures (k and l).<sup>33</sup> Adapted with permission from the Wiley, the IOP science, the Royal Society of Chemistry, and the American Chemical Society.

the growth process was preferentially enhanced, but not the nucleation process, by increasing the initial the POM concentration at a given molar ratio, and the size of the nanomaterials consequently increased.

In another study, a self-assembled complex based on POMs and a cationic surfactant was applied to synthesize flower-like gold NPs (Figure 4(h)).<sup>31</sup> The assemblies were formed by electrostatic combination between hydrogen atoms of the N—H groups of the cationic surfactant and oxygen atoms, which was supported by NMR and IR analysis. The assemblies served as a soft template, while the POMs formed the NPs under UV irradiation. The synthesized flower-like NPs showed a high peak current and the unique redox signals of POMs in cyclic voltammogram analysis, and this suggested that they have potential for application as an electrocatalyst with synergistic electrocatalytic activity.

Kida studied the synthesis of gold nanosheets at an aqueous–organic two-phase interface using POMs as a reducing and stabilizing agent (Figure 4(i) and (j)).<sup>32</sup> Moreover, it was demonstrated that the POMs preferred to absorb onto the gold {111} plane than other planes, so the gold nuclei grew along the {110} or {100} planes, as evidenced by XRD analysis of the gold nanosheets. Similar results were obtained in the synthesis of bamboo like-gold micro/nanostructures mediated by vanadium mixed-valence POMs (Figure 4(k) and (l)).<sup>33</sup> In this report, prominent growth on the {111} surface was also confirmed by XRD analysis.

**Palladium Nanomaterials.** Several studies have reported the synthesis of palladium nanomaterials using POMs and the good catalytic ability of the synthesized nanomaterials in various reactions.

Sastry and coworkers described the synthesis of hydrophobized palladium NPs by photochemically reduced Keggin-type POMs (Figure 5(a)). The fabricated NPs showed ability as a multifunctional catalyst for Heck, ring-opening, and acylation reactions.<sup>34</sup> Furthermore, the palladium NPs fabricated by using Mo mixed-valence POMs without photocatalytic reduction also showed good catalytic capability in the electrocatalytic oxidation reactions of methanol and ethanol (Figure 5(b)). The presence of the POMs in the synthesized NPs was demonstrated through Fourier transform infrared (FT-IR) or X-ray photoelectron spectroscopy (XPS) analysis in both studies, indicating the POM stabilization of the NPs.<sup>35</sup>

Zhang *et al.* demonstrated the self-organization behaviors of POM-coated palladium NPs, in which Dawson-type V-substituted POMs served as the reducing and stabilizing agent.<sup>23</sup> The size of the NPs could be tuned by the molar ratio of palladium salt to POMs up to some point. When the molar ratio passed that point, two different size modes were observed by dynamic light scattering (DLS) analysis. These nonsimilar modes were identified as single-palladium NPs and their self-assembled blackberry-like structures (Figure 5(c)). It was revealed that counterion-mediated attraction based on the partially hydrophilic surface of the POM-stabilized NPs led to the formation of these supramolecular structures.

In another study, the preparation of palladium NPs by the hydrogenation of non-organometallic Pd<sup>II</sup> derivatives of POM was reported (Figure 5(d)).<sup>36</sup> The stability of the fabricated NPs was attributed to the stability of the complexing POMs in aqueous solution. The POMs were maintained during hydrogenation, which means the selective reduction of Pd<sup>II</sup>, as evidenced by XPS, NMR, and Raman studies.

**Platinum Nanomaterials.** The facile synthesis of platinum NPs through various Mo mixed-valence POMs and their electrocatalytic power for alcohol oxidation were described (Figure 6(a)).<sup>35</sup> The size of the NPs could be controlled by adjusting the molar ratio of the metal salt to POMs. The synthesized platinum NPs showed not only good ability in the oxidation of methanol and ethanol but also resistance to poisoning during methanol oxidation. Additionally, platinum nanospheres synthesized through reduction by chemically reduced POMs and electrochemically reduced POM-mediated platinum NPs were reported (Figure 6(b)–(d)).<sup>18,37</sup> The POMs remained on the surface of the NPs after the formation of NPs, which was verified by XPS, IR, UV–vis and electrochemical analysis. The synthesized nanomaterials also showed improved electrocatalytic activities in the oxidation of alcohol in comparison with commercial platinum catalysts.

**Other Metals Nanomaterials.** The synthesis of selenium and tellurium nanomaterials by the Keggin structure POMs has been proposed (Figure 7). Selenium NPs were synthesized in the presence of photochemically reduced POMs, and the POM-stabilized selenium NPs were confirmed by energy-filtered transmission electron microscopy (EFTEM) analysis, which showed that the NPs were enclosed by the POMs.<sup>38</sup> The size of the selenium NPs was also tunable by controlling the ionic strength of the solutions and by adjusting the molar ratio

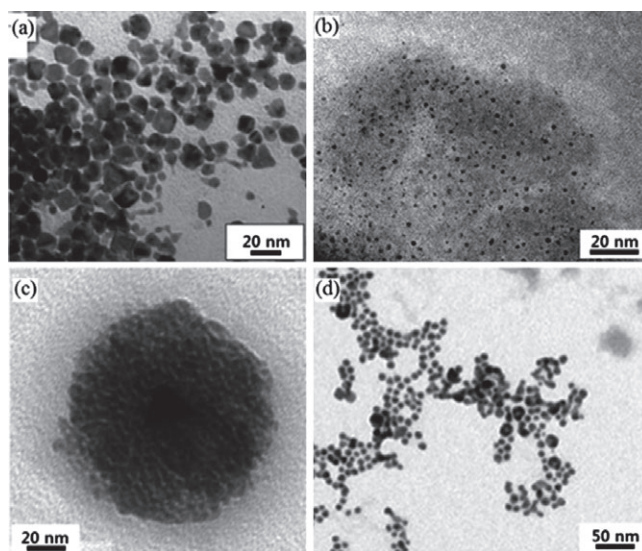


**Figure 5.** POM-assisted Pd nanomaterials. TEM images of (a) hydrophobized Pd NPs,<sup>34</sup> (b) NPs,<sup>35</sup> (c) hollow supramolecular structures of Pd aggregates referred to as “blackberry” structures,<sup>23</sup> and (d) NPs obtained by hydrogenation.<sup>36</sup> Adapted with permission from the American Chemical Society and the Royal Society of Chemistry.

between the metal salt and POMs, as was seen in several studies.

POM-assisted tellurium nanotubes with a hexagonal or sloping cross section were synthesized under hydrothermal conditions, in which POMs were reduced through 2-propanol as a sacrificial reagent without a photochemical reduction

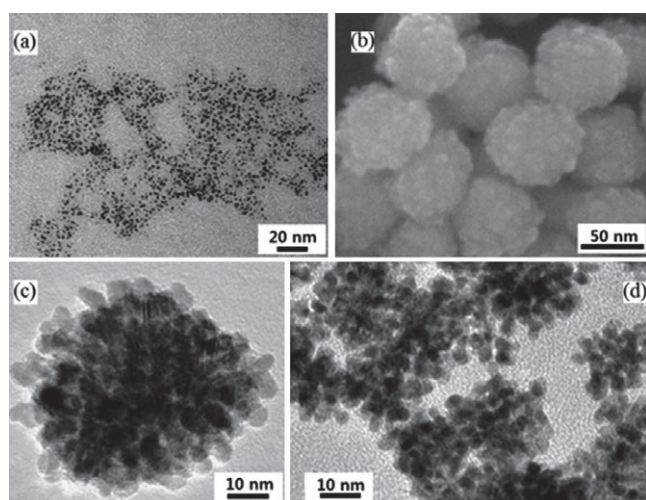


**Figure 6.** POM-assisted Pt nanomaterials. (a) TEM image of NPs synthesized in water at room temperature.<sup>35</sup> Low-magnification SEM image (b) and high-magnification TEM image (c) of nanospheres.<sup>37</sup> (d)  $\text{H}_{12}\text{W}_{12}$ -Pt NPs.<sup>18</sup> Adapted with permission from the American Chemical Society, Elsevier, and the Royal Society of Chemistry.

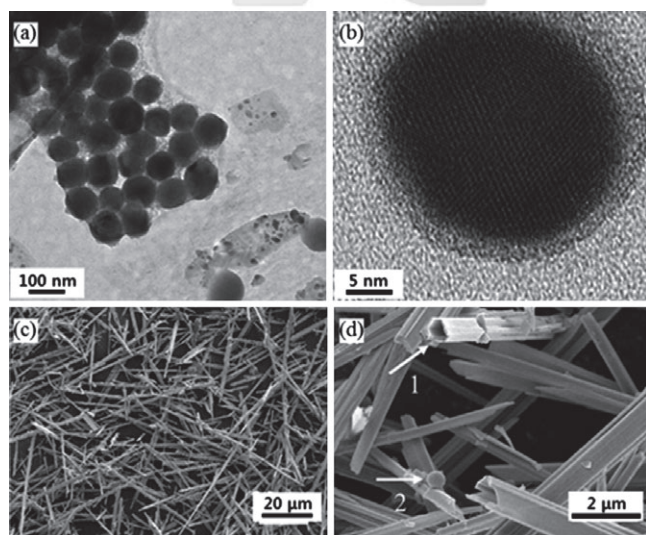


**Figure 7.** POM-assisted Se and Te nanomaterials. (a, b) TEM images with different magnifications of selenium NPs. (c, d) Low-magnification and high-magnification SEM image of tellurium nanotubes. Some tellurium nanotubes show hexagonal cross sections (as indicated by the arrow 1 in (d)). Part figure (d) shows that some tiny spherical NPs can be found on the surface of the sample (as indicated by arrow 2). Adapted from Refs 38 and 39 with permission from Elsevier, and the Wiley.

process.<sup>39</sup> The molar ratio of metal ions to POMs affected the morphology of the tellurium nanotubes rather than the size and growth of the nanotubes, which occurred along the [001] direction, as confirmed by XRD, TEM, and selected area diffraction (SAED) analysis.

### Synthesis of Bimetallic Nanomaterials by POMs

The synthesis of bimetallic nanomaterials has been intensively studied because of the synergetic effects of their catalytic performance compared with their monometallic counterparts.<sup>40</sup> The POM-assisted synthesis of nanomaterials was also investigated. Sastry and coworkers reported the preparation of Au core-M shell (M: Ag, Pd, and Pt) bimetallic NPs (Figure 8).<sup>41,42</sup> A two-step UV irradiation method was adopted for the synthesis of core-shell NPs as shown in Figure 9. The gold cores were obtained by photochemically reduced Keggin-type POMs, and then the formation of the shells occurred under UV irradiation through selective reduction on the POM-bound surface of the gold core. Although significant research is still required, bimetallic NPs using POMs are expected to show interesting properties.

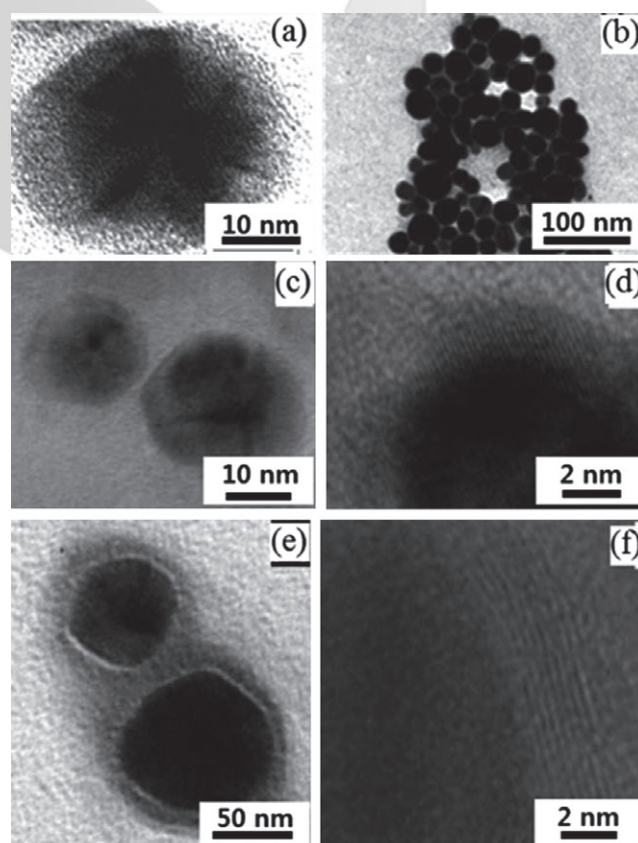


**Figure 8.** POM-assisted bimetallic NPs. (a) High- and (b) low-resolution TEM images of Au core-Ag shell NP. (c) High- and (d) low-resolution TEM images of Au core-Pd shell NP. (e) High- and (f) low-resolution TEM images of Au core-Pt shell NP. Adapted from Refs 41 and 42 with permission from the American Chemical Society and the Royal Society of Chemistry.

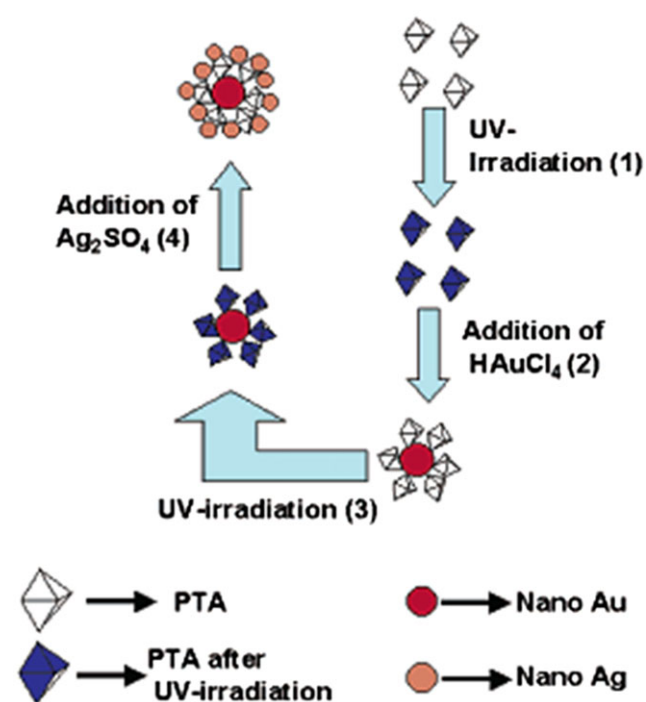


**Figure 9.** Scheme of the Keggin ion-mediated synthesis of Au core-Ag shell NPs. For simplicity, Keggin ions are shown as octahedral particles. Adapted from Ref. 41 with permission from the American Chemical Society.

### POM-assisted Nanohybrid Materials

POMs have been introduced in the preparation of various nanohybrid materials owing to their ability to synthesize NPs with good catalytic properties. They can serve not only as reducing and stabilizing agents during the formation of NPs but also as bridging molecules between the NPs and other components. POM-assisted nanohybrid materials were found to have synergistic effects on each component in terms of the catalytic performance and long-term stability of the as-synthesized nanomaterials.

The decoration of carbonaceous materials such as carbon nanotubes (CNTs) and graphene with various metal NPs by using POMs has been reported recently. For the first time, Li *et al.* proposed a method to prepare POM-stabilized Au NPs decorated CNTs without the addition of other toxic organic molecules (Figure 10(a)), and demonstrated the role of the POMs as bridging molecules.<sup>24</sup> A three-component nanohybrid was obtained by photochemically reduced Keggin-structure POMs at room temperature, as shown in Figure 10(b). Single-crystalline Au NPs were well dispersed on the walls of the CNTs and were surrounded with the POMs, indicating that the POMs stabilized the NPs (Figure 10(c)). The size and the coverage of the NPs on the CNTs were tunable by modifying the initial concentrations of both POMs and the metal salt and the oxidation degree of CNTs, respectively. The decoration process suggested that the hydrogen bonds between the POMs and carboxylic groups on the side walls

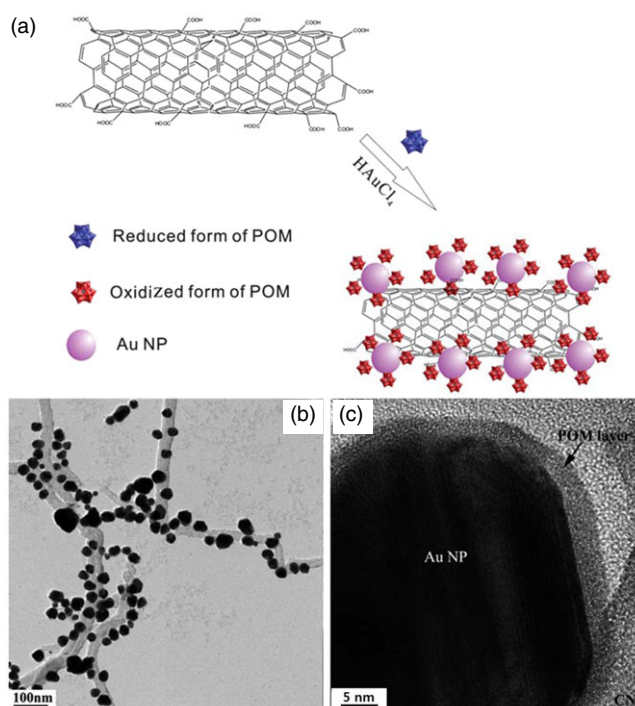


**Figure 10.** (a) Schematic illustration of the experimental procedure in which POMs serve as the reducing agent as well as encapsulating and bridging molecules. TEM images of (b) Au NP@POM-CNT composites and (c) magnified image of one Au NP on a single CNT. Adapted from Ref. 24 with permission from the Royal Society of Chemistry.

of the CNTs led to the attachment of the Au NPs, and the presence of hydrogen bonding was confirmed by IR and Raman analysis. The synthesized nanohybrid showed high photocatalytic activity toward the photodegradation of rhodamine B because of the synergistic effect of the three components. In addition to this study, there have been many reports on the synthesis of POM-mediated NP/carbon-based hybrid materials.<sup>25,43–45</sup>

### Conclusions

In this review, we described the synthesis of various metal nanomaterials by using POMs as stabilizing, reducing, and bridging molecules without the introduction of toxic organic materials. POMs can be reduced in a variety of ways, and the reduced POMs can be reoxidized by reducing the metal ions without changing their structures in both electron transfer processes. The as-synthesized nanomaterials were surrounded with POMs, which have been shown to affect the stability and the dispersion of nanomaterials for a long time. In particular, POM-stabilized nanomaterials have shown enhanced catalytic performance in many studies because of the synergistic effects with POMs, which have properties of high activity and reversible multielectron redox transformations during the catalytic reaction. However, the shapes of the nanomaterials synthesized through POMs are mainly spherical, and it is necessary to investigate the shape control of nanomaterials. Moreover,

the detailed mechanisms of the formation of nanomaterials and interactions by POMs remain unclear. Therefore, it is necessary to intensively study this field to advance the preparation of POM-mediated nanomaterials and enable their application in a wide range of applications in fields such as catalysis and materials science.

**Acknowledgment.** Publication cost of this paper was supported by the Korean Chemical Society.

### References

1. D. L. Long, R. Tsunashima, L. Cronin, *Angew. Chem. Int. Ed.* **2010**, *49*, 1736.
2. J. Y. Niu, S. W. Zhang, H. N. Chen, J. W. Zhao, P. T. Ma, J. P. Wang, *Cryst. Growth Des.* **2011**, *11*, 3769.
3. I. V. Kozhevnikov, *Chem. Rev.* **1998**, *98*, 171.
4. E. Rafiee, S. Tangestaninejad, M. H. Habibi, V. Mikhani, *Bull. Korean Chem. Soc.* **2004**, *25*, 599.
5. J. T. Rhule, C. L. Hill, D. A. Judd, R. F. Schinazi, *Chem. Rev.* **1998**, *98*, 327.
6. Y. P. Jeannin, *Chem. Rev.* **1998**, *98*, 51.
7. X. López, J. J. Carbó, C. Bo, J. M. Poblet, *Chem. Soc. Rev.* **2012**, *41*, 7537.
8. M. Ammam, *J. Mater. Chem. A* **2013**, *1*, 6291.
9. D. E. Katsoulis, *Chem. Rev.* **1998**, *98*, 359.
10. A. P. Alivisatos, P. F. Barbara, A. W. Castleman, J. Chang, D. A. Dixon, M. L. Klein, G. L. McLendon, J. S. Miller, M. A. Ratner, P. J. Rossky, S. I. Stupp, M. E. Thompson, *Adv. Mater.* **1998**, *10*, 1297.
11. A. L. Efros, M. Rosen, *Annu. Rev. Mater. Sci.* **2000**, *30*, 475.
12. A. Z. Moshfegh, *J. Phys. D Appl. Phys.* **2009**, *42*, 233001.
13. B. Hvolbaek, T. V. W. Janssens, B. S. Clausen, H. Falsig, C. H. Christensen, J. K. Nørskov, *Nanotoday* **2007**, *2*, 14.
14. X. Michalet, F. F. Pinaud, L. A. Bentolila, J. M. Tsay, S. Doose, J. J. Li, G. Sundaresan, A. M. Wu, S. S. Gambhir, S. Weiss, *Science* **2005**, *307*, 538.
15. A. Z. Wang, R. Langer, O. C. Farokhzad, *Annu. Rev. Med.* **2012**, *63*, 185.
16. M. A. Hahn, A. K. Singh, P. Sharma, S. C. Brown, B. M. Moudgil, *Anal. Bioanal. Chem.* **2011**, *399*, 3.
17. L. Chalkley, *J. Phys. Chem.* **1952**, *56*, 1084.
18. T. Hsu-Yao, K. P. Browne, N. Honesty, Y. J. Tong, *Phys. Chem. Chem. Phys.* **2011**, *13*, 7433.
19. A. V. Gordeev, N. I. Kartashev, B. G. Ershov, *High Energ. Chem.* **2002**, *36*, 75.
20. J. Yuan, Y. Chen, D. Han, Y. Zhang, Y. Shen, Z. Wang, L. Niu, *Nanotechnology* **2006**, *17*, 4689.
21. M. T. Pope, *Inorg. Chem.* **1972**, *11*, 1973.
22. I. A. Weinstock, *Chem. Rev.* **1998**, *98*, 113.
23. J. Zhang, B. Keita, L. Nadjo, I. M. Mbomekalle, T. B. Liu, *Langmuir* **2008**, *24*, 5277.
24. S. Li, X. Yu, G. Zhang, Y. Ma, J. Yao, B. Keita, N. Louis, H. Zhao, *J. Mater. Chem.* **2011**, *21*, 2282.
25. R. J. Liu, X. L. Yu, G. J. Zhang, S. J. Zhang, H. B. Cao, A. Dolbecq, P. Mialane, B. Keita, L. Zhi, *J. Mater. Chem. A* **2013**, *1*, 11961.
26. A. Troupis, A. Hiskia, E. Papaconstantinou, *Angew. Chem. Int. Ed.* **2002**, *41*, 1911.
27. G. Zhang, B. Keita, A. Dolbecq, P. Mialane, F. Sécheresse, F. Miserque, L. Nadjo, *Chem. Mater.* **2007**, *19*, 5821.
28. C. Marchal-Roch, C. R. Mayer, A. Michel, E. Dumas, F. X. Liu, F. Secheresse, *Chem. Commun.* **2007**, 3750.
29. L. Liu, C. He, J. Li, J. Guo, D. Yang, J. Wei, *New J. Chem.* **2013**, *37*, 2179.
30. G. Zhang, B. Keita, R. N. Biboum, F. Miserque, P. Berthet, A. Dolbecq, P. Mialane, L. Catala, L. Nadjo, *J. Mater. Chem.* **2009**, *19*, 8639.
31. H. Li, Y. Yang, Y. Wang, W. Li, L. Bi, L. Wu, *Chem. Commun.* **2010**, *46*, 3750.
32. T. Kida, *Langmuir* **2008**, *24*, 7648.
33. Y. Y. Bao, B. Wang, R. Q. Meng, L. H. Bi, L. X. Wu, *CrystEngComm* **2012**, *14*, 1550.
34. S. Mandal, A. Das, R. Srivastava, M. Sastry, *Langmuir* **2005**, *21*, 2408.
35. B. Keita, G. Zhang, A. Dolbecq, P. Mialane, F. Sécheresse, F. Miserque, L. Nadjo, *J. Phys. Chem. C* **2007**, *111*, 8145.
36. R. Villanneau, A. Roucoux, P. Beaunier, D. Brouri, A. Proust, *RSC Adv.* **2014**, *4*, 26491.
37. G. Sun, Q. Li, R. Xu, J. Gu, M. Ju, E. Wang, *J. Solid State Chem.* **2010**, *183*, 2609.
38. T. Triantis, A. Troupis, E. Gkika, G. Alexakos, N. Boukos, E. Papaconstantinou, A. Hiskia, *Catal. Today* **2009**, *144*, 2.
39. L. Zhang, C. Wang, D. Y. Wen, *Eur. J. Inorg. Chem.* **2009**, *22*, 3291.
40. N. Toshima, T. Yonezawa, *New J. Chem.* **1998**, *22*, 1179.
41. S. Mandal, P. R. Selvakannan, R. Pasricha, M. Sastry, *J. Am. Chem. Soc.* **2003**, *125*, 8440.
42. S. Mandal, A. B. Mandale, M. Sastry, *J. Mater. Chem.* **2004**, *14*, 2868.
43. R. Liu, S. Li, X. Yu, G. Zhang, S. Zhang, J. Yao, L. Zhi, *J. Mater. Chem.* **2012**, *22*, 3319.
44. R. Liu, S. Li, X. Yu, G. Zhang, Y. Ma, J. Yao, *J. Mater. Chem.* **2011**, *21*, 14917.
45. R. Liu, S. Li, X. Yu, G. Zhang, S. Zhang, J. Yao, B. Keita, L. Nadjo, L. Zhi, *Small* **2012**, *8*, 1398.